Extended-Nanofluidics: Fundamental Technologies, Unique Liquid Properties, and Application in Chemical and Bio Analysis Methods and Devices

ARTICLE *in* ANALYTICAL CHEMISTRY · APRIL 2014

Impact Factor: 5.64 · DOI: 10.1021/ac4026303 · Source: PubMed

5 AUTHORS, INCLUDING:

Yutaka Kazoe
The University of Tokyo
58 PUBLICATIONS **243** CITATIONS
SEE PROFILE

Yuriy Pihosh
The University of Tokyo
56 PUBLICATIONS **315** CITATIONS
SEE PROFILE

analytical chemistry

Feature

pubs.acs.org/ac

Extended-Nanofluidics: Fundamental Technologies, Unique Liquid Properties, and Application in Chemical and Bio Analysis Methods and Devices

Engineering using liquids confined in channels 10−1000 nm in dimension, or "extended-nanofluidics," is the next target of microfluidic science. Liquid properties at this scale were unrevealed until recently because of the lack of fundamental technologies for investigating these ultrasmall spaces. In this article, the fundamental technologies are reviewed, and the emerging science and technology in the extended-nanospace are discussed.

Kazuma Mawatari,[†,‡] Yutaka Kazoe,[†,‡] Hisashi Shimizu,[†,‡] Yuriy Pihosh,[†,‡] and Takehiko Kitamori*[,†,‡]

[†]Department of Applied Chemistry, School of Engineering, The University of Tokyo, 7-3-1 Hongo, Bunkyo, Tokyo 113-8656, Japan

[‡]CREST, Japan Science and Technology Agency, 5, Sanbancho, Chiyoda, Tokyo 102-0075, Japan

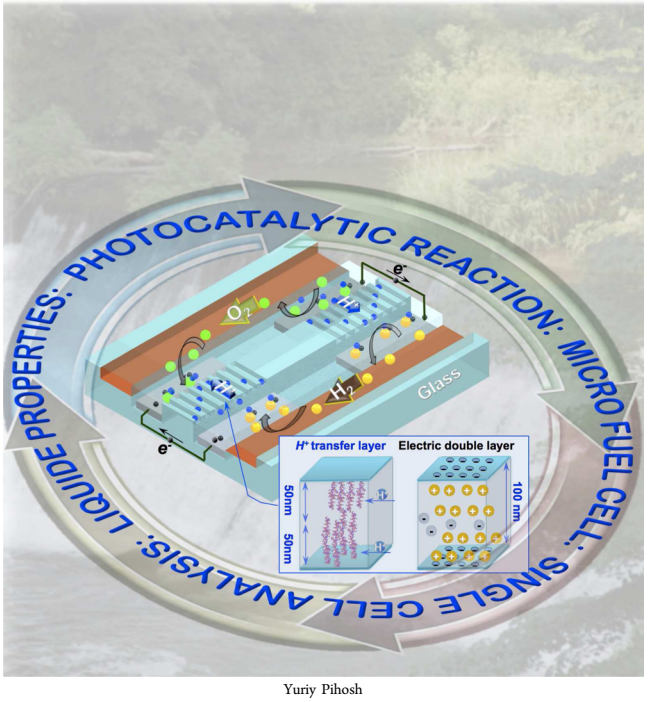

Yuriy Pihosh

Microfluidic technologies utilizing size-regulated micro-spaces, typically 10−100 μm (Figure 1), have developed very rapidly over the past 2 decades. In the early 1990s, the concept of a "micro total analysis system," or μTAS, was proposed by Manz's group.[1] The basic technologies at that time were electrophoretic separation and laser-induced fluorescence (LIF) detection. The applications were mainly DNA or protein separation and analysis. High performances were demonstrated in ultrasmall fluid volumes (nanoliter to picoliter) and very fast analysis times (seconds) were realized by utilizing the characteristics of the microspaces. However, the technologies involved limited the applications to the separation of DNA and proteins.

In the 2000s, the general concepts and technologies were proposed to realize the general integration of chemical processes in microfluidic chips. These concepts included micro unit operations (MUOs) and continuous flow chemical processing (CFCP).[2] The bulk-scale chemical operations were replaced by MUOs, and the different MUO regions were connected to each other in parallel and in series by CFCP channels, like an electric circuit. Pressure-driven multiphase microflows were advanced as fluidic control methods. Parallel flow and droplet flow were developed using surface chemical modification, control of channel size, and flow velocity.[3]

In addition to these fluidic control methods, other fundamental technologies were developed, such as detection technologies (optical, electrochemical, and via connection to conventional analytical instruments), fabrication materials and methods (silicon, glass, polymer, ceramics), and surface properties control methods (hydroaffinity, biomolecule, cell, catalyst). These technologies allowed for the treatment of various analytes (neutral or charged species), solvents (water or organic), and phases (gas, liquid, solid, and supercritical) in the microspaces, and the applications in the analytical and chemical synthesis fields expanded rapidly. Superior performance in comparison with bulk-scale operations was demonstrated: higher speeds, smaller sample and reagent volumes, easier operations, higher functionality, and more compact instrumentation. Currently, the microfluidics field is expanding in two directions: (1) the development of new applications involving living cells and (2) commercialization by the development of practical microsystems (e.g., microimmunoassay systems[4]).

Recently, the spaces involved have been scaled down even further, to sizes on the order of 10−1000 nm. We call these "extended-nanospaces," to reinforce the notion that the length scales they incorporate differ from those of conventional nanotechnologies that involve smaller length scales of 1−10 nm (e.g., carbon nanotube and mesoporous materials). The apparent merit for analytical technologies is that the volume of the extended-nanospaces (femtoliter to attoliter) is smaller than that of a single cell (~picoliter). Currently, biologists are emphasizing the importance of single cell analytical techniques, for protein expression analyses that reflect the heterogeneity of

Published: April 1, 2014

   dx.doi.org/10.1021/ac4026303 | *Anal. Chem.* 2014, 86, 4068−4077

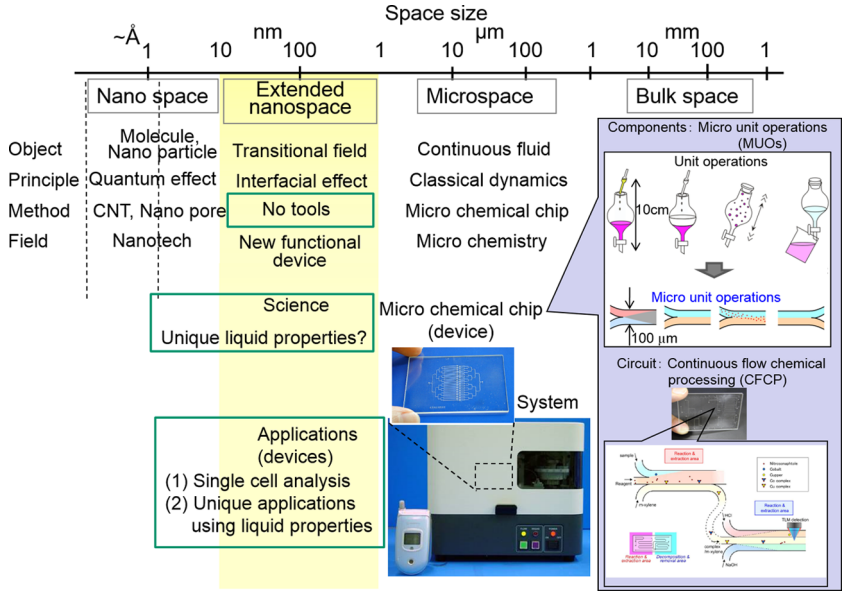

Figure 1. Size hierarchy of fluidic spaces; the extended-nanospace is intermediate to the micro- and nanospaces.

individual cells in particular.[5] Many researchers in microfluidics have attempted to develop analysis methods at the single-cell level using microspaces, but it was difficult because the volume of a single cell (picoliter) is comparable to (or smaller than) that of the microspace (picoliter to nanoliter). Extended-nanospaces have the potential to realize these next generation analytical tools in the biological sciences. In addition, the small size of the spaces allows many unique applications such as single DNA digestion mapping[6] and new separation modes.[7] In terms of electric double-layer effects, the characteristic dimension of the space is comparable to the Debye length, so surface charges will have a significant influence on the ionic distribution and concentration. Utilizing these surface effects, unique chemical operations have been developed such as ion concentration[8] and rectification.[9]

Another merit of these spaces is the unique liquid properties that can be realized. The extended-nano space is a transitional "mesoscopic" area that bridges the gap between isolated molecules and continuum liquids, whose properties are expected to be altered by the surface properties. Most research has focused on nanospaces with dimensions 1−10 nm, which are comparable in scale with individual molecules. Unique properties of molecules at the solid/liquid interface, called the adsorption layer, were reported. The small number of the molecules confined in the nanospaces makes numerical simulation relatively easy, and many methods have been developed that incorporate fundamental molecular mechanics or quantum mechanics. These results support the notion of properties changes in the adsorption layer. This combination of experimental and theoretical approaches has convinced researchers that the molecular behaviors differ under these conditions.

Despite these molecule-level advances, there have been almost no reports on the properties of continuum liquids in extended-nanospaces. One of the reasons for this is the lack of research tools. Extended-nanospaces are 3 orders of magnitude smaller than microspaces, even smaller than the wavelength of visible light. This complication is why the application of the fundamental technologies developed for microfluidics could not be applied. With respect to numerical simulation, the spaces were too large for calculations involving the entire volume, even using current supercomputers. To resolve this situation, experimental approaches were undertaken, aimed at developing the fundamental technologies. Initially, only electrophoresis was performed because of the simpler fluidics of operation, and researchers demonstrated unique chemical operations utilizing the effect of the surface charge. Following these results, novel fundamental techniques for general chemistry in the extended-nanospaces have been developed. Along with this technological progress, many unique liquid properties were found, and these were quite different from the bulk-scale liquid properties. On the basis of the findings, the relationship between the electric double-layer (EDL) effects and these found liquid properties is being investigated. In addition, these unique liquid properties have been utilized to develop novel functional devices based on principles which were quite difficult to realize in microspaces. The science and technology of the emerging research field surrounding extended-nanospaces is expected to provide novel analytical methods for chemistry and biology.

In this review, we briefly survey the state of the art of the fundamental technologies involving extended-nanospaces: nanofabrication, nanofluidic control, and detection technologies.[10,11] Detailed explanations of these technologies are avoided because of the limited space (refer to the reviews), and the important differences with respect to microspaces are emphasized. We also summarize the unique liquid properties and discuss the liquid model. We attempt to investigate these properties systematically by considering the common factors involved in the properties changes and discussing the generality of the phenomena. The electric double-layer model, a well-established theory describing the properties of liquids near interfaces at a scale of 10−1000 nm, is also considered. Finally, applications of extended-nanospaces are illustrated in which the characteristics of the extended-nanospace were utilized: small size, surface effects, and unique liquid properties. The information presented in this feature article provides a condensed overview of the recent science and technology of extended-nanospaces and will help new researchers in affected fields to understand the current research trends.

dx.doi.org/10.1021/ac4026303 | *Anal. Chem.* 2014, 86, 4068−4077

FUNDAMENTAL TECHNOLOGIES

Top-down Fabrication, Bottom-Up Fabrication, and Substrate Bonding. Extended-nanospaces have been utilized in conventional chemical operations: filtration by membrane and liposome. However, the sizes of the spaces were not well controlled or the spaces were closed off. To reveal the properties of liquids in these spaces, well-controlled extended-nanochannels are essential. For this purpose, many fabrication methods have been established, both top-down and bottom-up. For extended-nanofluidic systems, top-down fabrication has been utilized for size control in the range 10−1000 nm.

Typical top-down fabrication methods involve patterning and etching processes. Photolithography, in which a photomask is employed to make microscale photoresist patterns, is one of the most popular patterning methods in microfluidics. By combining photolithographic and dry etching methods (e.g., inductively coupled plasma etching, reactive-ion etching, and fast-atom-beam etching), many nanochannels with microscale width and nanoscale depth were fabricated. The fabrication process was relatively easy, and most of the researchers were able to utilize the nanochannels. In order to fabricate nanochannels with nanoscale dimensions in width and depth, electron beam (EB) lithography and dry etching methods were utilized (Figure 2). Tsukahara et al. reported nanochannel fabrication on a fused-silica substrate that combined EB lithography and inductively coupled plasma etching methods.[12] For realizing channels with high aspect ratios (>5), planar-type neutral loop discharge (NLD) etching was conducted on a fused silica substrate.[13] Focused ion beam (FIB) etching can realize direct patterning and etching at the nanometer scale, and it has been employed in nanochannel formation.[14] The disadvantage was the long fabrication time.

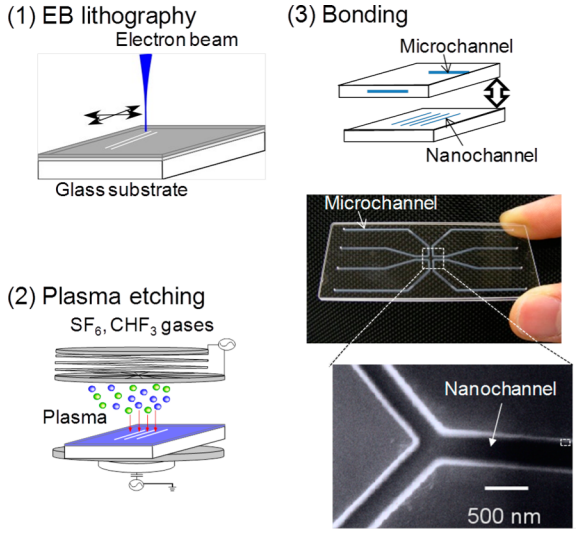

Figure 2. Representative top-down nanofabrication process.

Molding processes were a popular method for making channels in soft materials such as plastics, and these processes were also applied to nanochannel fabrication in plastic materials. A representative technique was nanoimprint lithography (NIL), which used thermoplastic polymers such as polymethylmethacrylate (PMMA), polycarbonate (PC), and polydimethylsiloxane (PDMS). After making the mold, nano-channels were formed by various NIL methods: thermal NIL, photocuring NIL, and soft NIL.[15−19] The advantage of these methods was the large quantities of nanochannels that could be fabricated by repeating the molding process on different substrates. However, for general chemistry applications involving both aqueous and organic solvents, plastic materials tend to have low stability and glass materials are good candidates for performing basic science in the extended-nanospaces.

Top-down fabrication methods were successfully developed to form nanochannels on both hard and soft materials. However, top-down fabrication schemes alone are not sufficient to provide various chemical functions; bottom-up fabrication principles are also essential. In particular, nanochannels have extremely large surface-to-volume ratios and functionalization by partial surface modification is a key technology. However, partial surface modification is difficult in extended-nanospaces. One of the reasons is related to the substrate-bonding method. As a general fluidic control method, pressure-driven flow was utilized. High pressures (~megapascals) were required as a consequence of the small size: to attain constant linear flow velocity, the required pressure is proportional to the square of the channel size. In order to prevent leakage at these high pressures, strong bonding methods were necessary. For glass/glass bonding, a thermal bonding process was developed in which fused-silica substrates were bonded at 1060 °C.[20] Since the partial modifications are lost during high temperature heating, the modifications should be performed after the bonding process; this is difficult due to the small spaces involved. Only one group has reported a local DNA immobilization method using polyethyleneglycol-benzophenone as a photolinker.[21] In order to solve this technological

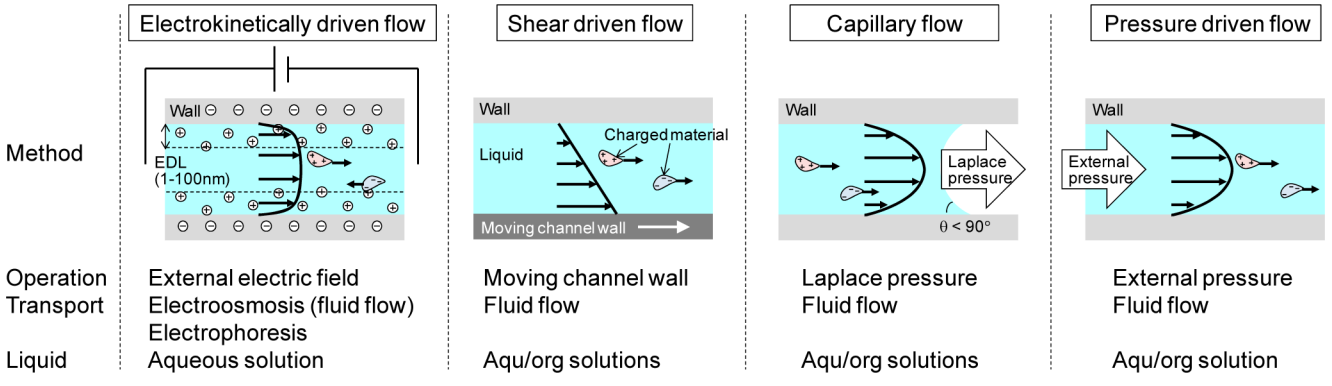

Figure 3. Summary of fluidic control methods in extended-nanochannels.

dx.doi.org/10.1021/ac4026303 | *Anal. Chem.* 2014, 86, 4068−4077

problem, Xu et al. developed a low temperature glass/glass bonding method.[22] A glass substrate was treated by oxygen plasma and fluorine atoms, and bonding at low temperature (<100 °C) was realized. These low temperature processes will permit the functionalization of nanochannels using bottom-up techniques. Partial antibody patterning in devices fabricated by combining the low-temperature bonding method and amino-group patterning with vacuum ultraviolet light was reported.

Fluidic Control Methods. Fluidic control is a fundamental component of extended-nanoscale fluid engineering for realizing novel devices. Manipulation of liquids with ultrasmall volumes (attoliter to femtoliter) in size-regulated extended-nanochannels, in which the flow rate is in order of 1 pL/min, is required. Generally, in fluidic control by pressure driven flows with no-slip boundaries, the fluidic resistance of extended-nanochannels is high as a result of the increased surface-to-volume ratio. For example, the pressure ΔP required for a flow velocity U is given by the Hagen−Poiseuille equation: $\Delta P = 32\mu LU/d^2$, where μ is the viscosity, L is the channel length, and d is the channel diameter. For a flow rate of 1 mm/s in an extended-nanochannel of diameter 100 nm and length 1 mm, ΔP is on the order of 1 MPa; this is 10^6 times the pressure required in a 100 μm diameter microchannel. Therefore, the strategy for fluidic control in extended-nanochannels is to avoid or mitigate this high fluidic resistance by using other principles or to achieve system pressures of several megapascals. Several methods have been developed for doing this, as summarized in Figure 3.

The most commonly used fluidic control method is electrokinetically driven flow, generated by the application of external electric fields. Electrokinetically driven flows can avoid the high fluidic resistance of extended-nanochannels by electrically driving the fluid near the channel wall. The driving force in the fluid is provided by the drag of wall-adjacent ions in an electric double-layer region, i.e., an ion screening layer of 1−100 nm thickness which cancels the surface charge. When the external electric field is applied, the ions in the EDL are driven, and fluid flow is induced. Additionally, charged species in extended-nanochannels are transported at different velocities in different directions depending on their charge, which is also known as electrophoresis. Since the external electric fields can be controlled through electrodes integrated or inserted in microfluidic devices, operation is simple. Previous studies have achieved fluid transport, switching, and electrophoretic separation in extended-nanochannels.[19,23−26] However, the methods are only applicable in aqueous solutions incorporating ions. In addition, uniform transport of suspended materials, which is one of most important factors for chemical operations, is difficult as a result of electrophoretic effects. Therefore, the application of electrokinetically driven flow is limited.

Fluidic control by shear driven flow is another way to avoid the high fluidic resistance by mechanically driving the near-wall fluid, as proposed by Desmet et al.[27−29] Flow is induced by moving a wall of the fluidic channel. A flat plate, rotation disk, or flexible belt can be used as the moving wall. The fluid is driven by the viscous force, which induces a linear velocity profile, assuming that the fluid properties are uniform in the extended-nanochannel. In contrast to electrokinetically driven flow, flows of both aqueous and organic solutions can be realized, and the materials in the channel are transported uniformly. The method has achieved both basic fluid transport and chromatographic separation. However, nanofluidic devices incorporating moving wall systems are difficult to fabricate.

Flow control employing high (megapascal) driving pressures has also been developed. The most simple and easiest methods use the Laplace pressure derived from the surface tension, which is dominant in extended-nanospaces. From the Young−Laplace equation $\Delta P_L = 4\gamma \cos\theta/d$, where γ is the surface tension and θ is the contact angle, the Laplace pressure ΔP_L in an extended-nanochannel (d = 100 nm) with a completely wetting surface ($\theta \approx 0$) is on the order of 1 MPa. Previous studies have used capillary filling to drive the fluid in extended-nanochannels.[30,31] However, because the Laplace pressure is determined by the interfacial properties, the fluid flows are not adjustable during operation. Furthermore, these capillary methods are applicable only for wetting surfaces.

In order to achieve general chemical operations in extended-nanofluidic devices incorporating various materials and surfaces, fluidic control by application of external pressure is most effective, even in extended-nanospaces. As a result of the extremely high fluidic resistance and low flow rate, commercial syringe pumps, which are commonly used for microfluidic devices, do not provide the required pressures. Therefore, a pressure control system incorporated into the extended-nanofluidic device, in which the extended-nanochannels are connected to microchannels for sample injection, has been developed by Kitamori et al.[32,33] Liquid in the macroscopic reservoir is driven by air pressure, injected into microchannels, and from there introduced into the extended-nanochannels. In principle, the method is applicable to both aqueous and organic solutions. By using a cross-shaped extended-nanochannel, attoliter sample volumes have been realized.[34] The capability of the method for performing various chemical operations, such as simple mixing for reaction, immunoassay, and chromatography, has been demonstrated.[33,35,36]

Detection Methods. Detection is also an important and challenging issue in extended-nanospaces for two reasons. First, the number of analyte molecules decreases according to the decrease in volume. For instance, the volume of a 100 nm cube is 1 aL. When the concentration of an analyte is 1 μM, the number of analyte molecules in the cube is 0.6 molecules. This means single-molecule sensitivity is required in extended-nanospaces, with help of signal amplification techniques in some situations. Second, the scale of the extended-nanospace is nearly equal to, or shorter than, visible wavelengths of light. Therefore, optical detection methods utilizing geometrical optics, such as reflection and refraction, are of no use. Instead, wave optics effects, such as interference and diffraction, have advantages for detection in extended-nanospaces. In addition, ultrahigh resolution microscopic methods are required to obtain space-resolved information in extended-nanospaces. Thus, detection in extended-nanospaces is difficult compared to detection in microscale and bulk spaces. Removing samples from the extended-nanospaces and connecting them with other analytical instruments also require interfaces which can handle the extremely small volume. In this section, we focus on detection methods in extended-nanospaces and review the features and applications of individual methods.

Optical detection methods are highly compatible with micro- and nanofluidics because they make possible applications in confined spaces as well as the simplification and miniaturization of instruments and noninvasive measurement techniques. In particular, laser-induced fluorescence (LIF), which has single molecule sensitivity, is widely used.[37] To detect individual molecules, the most important consideration is improvement of the signal-to-background (S/B) ratio. The signal-to-noise (S/

dx.doi.org/10.1021/ac4026303 | Anal. Chem. 2014, 86, 4068−4077

Table 1. Summary of Unique Properties of Aqueous Solutions Discovered in Extended-Nanochannels

property	effect	channel material	space size (depth)	method
viscosity	1.4−4×	fused silica, SiO_2	25−1000 nm	capillary filling[30,31,48,49]
diffusion coefficient of macromolecules	1/5000−2/3	fused silica, SiO_2	50 nm, 260 nm	fluorescence observation of DNA and proteins[51,53]
flow rate of decane, ethanol, water	25−45×	carbon nanopipes	44 nm	mass monitoring by balance[54]
conductivity	20−25×	glass modified with $-SO_3H$ groups	50−1000 nm	current measurement[58]
dielectric constant	1/7−1/4	fused silica	330 nm, 580−800 nm	time-resolved fluorescence measurement,[30] streaming potential[63]
proton mobility	20×	fused silica	40−800 nm	NMR[64]
proton diffusion coefficient	8×	fused silica	180−330 nm	fluorescence microscopy[66]
hydrogen ion concentration	19×	fused silica	400 nm	STED microscopy[47]
enzyme reaction rate	2×	fused silica	340 nm	fluorescence microscopy[33]
dissociation of −SiOH group	enhanced	fused silica	580 nm	streaming current[66]
vapor pressure	lower than bulk theory	extended-nanopillar: fused silica	120−510 nm	microscopic observation[67]

N) ratio should be subsequently improved by increasing the gain of the detector. In conventional single molecule analyses using LIF, confocal microscopy was mainly used to detect the signal from analyte molecules in a particular focal volume and exclude the background originating from the out-of-focus regions of the solvent. Similarly, the use of extended-nanochannels improves the S/B ratio because the analyte molecule is confined in a space smaller than the wavelength. The combination of single molecule LIF and extended-nanospaces is frequently used in the analysis of stretched DNA molecules.[38]

On the other hand, detection of nonfluorescent molecules is more difficult, although the majority of molecules are nonfluorescent. As a sensitive detection method for nonfluorescent molecules, thermal lens spectrometry (TLS) has been developed and applied to various microfluidic analytical devices.[39] However, conventional TLS was not applicable to extended-nanospaces because its principle was based on refraction, a concept of geometrical optics. In order to solve this problem, a novel TLS method based on wave optics has been developed that can detect concentrations of 390 molecules in 250 aL.[40] Surface plasmon spectroscopy methods, such as surface plasmon resonance and surface-enhanced Raman spectroscopy are also useful for detecting nonfluorescent molecules.[41,42] The combination of surface plasmon techniques and extended-nanospaces permits the utilization of the whole fluidic channel as a detection field because the region of interaction between surface plasmons and analyte molecules is similar to a wavelength of the incident light.

Another method which is applicable to extended-nanospaces is electrical detection. When the size of the confining space is close to the size of the molecules, intrusion of an analyte molecule into the space leads to a significant change in electric properties, which enables sensitive detection.[43] In particular, ionic current blockade or resistive pulse sensing using nanopores has been actively investigated for single molecule analysis.[44] Although biological nanopores (e.g., α-Hemolysin) have been used in early research, solid-state nanopores have recently appeared, making integration possible in micro- and nanofluidic devices.[45] Next generation DNA sequencers are anticipated to use nanopores techniques.[46]

Finally, we mention the ultrahigh resolution techniques required to obtain spatially resolved information in extended-nanospaces. To acquire chemical information with resolutions less than the wavelength of light, scanning near-field optical microscopy (SNOM) is generally used, but SNOM cannot be applied to these confined spaces because of the use of physical probes. Therefore, some optical ultrahigh resolution techniques have been implemented for these purposes. For example, stimulated emission depletion (STED) microscopy was employed to measure the ion distribution in a 400 nm extended-nanochannel at a resolution of 87 nm.[47]

UNIQUE LIQUID PROPERTIES

Understanding the properties of liquids confined in extended-nanospaces is important to the basic science of extended-nanochemistry. Surface effects become significant in extended-nanospaces because of the increased surface-to-volume ratio, which is typically 1000 times higher than that of microspaces. In addition, considering the size of a water molecule (2.8 Å), the liquid confined in extended-nanospaces with sizes ranging from 10 nm (36 molecules) to 1000 nm (3600 molecules) is in a transitional regime between that of single molecules and that of the condensed phase. Therefore, liquid properties that are different from the bulk are expected. Some unique liquid properties demonstrated in extended-nanospaces as summarized in Table 1, and liquid models explaining the emergence of these properties are described below.

LIQUID PROPERTIES

Several research groups have reported unique fluidic properties in extended-nanochannels. Previous work has measured the capillary filling speed of water in glass extended-nanochannels and suggested higher viscosities of water (1.4−4 times as large) in glass extended-nanochannels compared with the bulk viscosities.[30,31,48,49] Tas et al. revealed that the increased viscosity in an extended-nanochannel was reduced by increasing the NaCl concentration and considered that the increased viscosity can be attributed to the effect of the electric double layer.[31] On the other hand, Hibara et al. and Haneveld et al. suggested that the increase in viscosity is related to the emergence of structured water in the glass nanochannels.[30,48] Most recently, Li et al. revealed an interesting trend of the increased viscosity: the water viscosity is significantly increased in square nanochannels (nanoscale width and depth) at sizes smaller than 1000 nm, while it is only slightly increased in plate nanochannels (microscale width and depth) at depths smaller than 50 nm.[49] In addition, a significant decrease in the diffusion

dx.doi.org/10.1021/ac4026303 | Anal. Chem. 2014, 86, 4068−4077

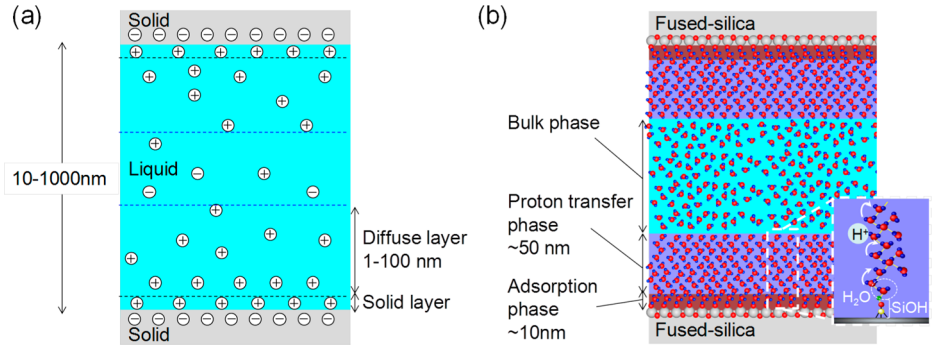

Figure 4. Schematic illustrations of the liquid model for extended-nanospaces. (a) Electric double layer in extended-nanospaces, which consist of the solid layer and diffuse layer. (b) Three-phase model of a liquid confined in an extended-nanospace, which consists of the adsorption phase, proton transfer phase, and bulk phase.

coefficients of fluorescent ions and macromolecules, probably to the result of interactions between molecules and surfaces, was suggested by fluorescence observations.[50−53] On the other hand, measurements of pressure driven flows in hydrophobic carbon extended-nanopipes showed higher flow rates than in the bulk, suggesting interactions between the hydrophobic surfaces and liquid.[54]

Electrical conductivity in extended-nanospaces, which is strongly related to ion behavior, has been studied.[55−57] The conductance of a KCl solution in an extended-nanochannel of 50 nm height was estimated from ac impedance measurements using platinum electrodes embedded in microchannels bridged with the nanochannels. The conductance decreased with decreasing KCl concentration, reaching a plateau for KCl concentrations below 10^{-4} M. This conductance plateau could be explained by increased proton conductivity in the extended-nanochannel.[55] Liu et al. measured the proton conductivity of an $HClO_4$ solution in extended-nanochannels using the electric current. The proton conductivity increased by a factor of 20−25 over that of the bulk because of the excess protons introduced by the dominant effect of the EDL in the extended-nanospace.[58]

The dielectric constants of liquids in extended-nanospaces, which are related to the liquid structure, have been studied by Kitamori et al. The time-resolved fluorescence measurements were conducted in a 330 nm extended-nanochannel filled with water. The results revealed a lower dielectric constant of water, which suggests a different liquid structure from the bulk.[30] From ac impedance measurements, the decrease in the capacitance related to the dielectric constant of liquid was also detected for a KCl solution in an extended-nanochannel.[59] Recently, streaming potential/current methods for extended-nanospaces have been developed by several groups.[60−62] The streaming potential/current is generated by counterions of the surface charges moving through the channel by pressure driven flow. Morikawa et al. developed a streaming potential/current system for extended-nanofluidic devices and established a measurement method for the dielectric constant of liquid in an extended-nanochannel. The results suggested a dielectric constant of water $^1/_4$ that of the bulk in fused-silica extended-nanochannels smaller than 800 nm.[62,63]

It has been unclear how the properties of liquid are affected in extended-nanospaces at the molecular level. Tsukahara et al. studied the molecular structure and dynamics of water and nonaqueous solvents confined in fused-silica extended-nanospaces using nuclear magnetic resonance (NMR).[12,64] The results suggested slower translational motions of water in extended-nanospaces but that the hydrogen bond structure and rotational motion were similar to the bulk. This change in the translational characteristics of H_2O can be attributed to protonic diffusion, invoking an excess proton hopping pathway along a linear O···H−O hydrogen bonding chain between adjacent water molecules. Further investigation revealed that the proton exchange rate of water molecules confined in an extended-nanospace is larger by a factor of more than 10 from that of bulk water because of the chemical exchange of protons between water and SiOH groups on glass surfaces. These unique properties could be observed for protic solvents but not in nonprotic solvents.

The knowledge obtained from these NMR measurements suggests unique water behavior related to the enhancement of proton hopping in extended-nanospaces; hence, the recent focus on proton behavior in extended-nanospaces. Mawatari et al. studied proton diffusion through fused-silica extended-nanochannels using a fluorescent pH indicator. The proton diffusion coefficient increase significantly to 8 times that of the bulk in a 180 nm fused-silica extended-nanochannel. These increases in proton diffusion coefficients are attributed to the domination of proton hopping by the Grotthuss mechanism.[65] Kazoe et al. measured the distribution of hydrogen ions as dissociated protons in a 400 nm fused-silica channel using STED microscopy. The hydrogen ion concentration is 19 times higher than in the bulk and is nonuniformly distributed in the extended-nanochannel.[47]

The unique water properties in extended-nanospaces are expected to affect reaction properties. Tsukahara et al. demonstrated an enzyme reaction in which the fluorogenic substrate TokyoGreen-β-galactoside is hydrolyzed to fluorescein derivative TokyoGreen and β-galactose by a β-galactosidase enzyme acting as a catalyst in a Y-shaped extended-nanochannel. The enzyme reaction rate was increased by a factor of about 2 compared with the bulk reaction. This acceleration of the reaction kinetics is attributed to the enhancement of proton mobility in water in an extended-nanospace.[33] Using the streaming current method, isoelectric points in extended-nanochannels fabricated from fused silica were measured. From the streaming current measurements, the isoelectric point in the silanol dissociation: $\equiv SiO^- + 2H^+ \Leftrightarrow \equiv SiOH_2^+$, which has been reported to be 2.6−3.2 in the bulk, can be estimated. The isoelectric point in microchannels was similar to the reported values, but in a 580 nm extended-nano channel it decreased to less than 2.0. From these results, the enhancement of proton dissociation in extended-nanospaces was suggested.[66]

dx.doi.org/10.1021/ac4026303 | Anal. Chem. 2014, 86, 4068−4077

The effects of these unique water behaviors on phase transitions have also been reported. Generally, when water is in confined geometries, the saturated vapor pressure is lower than that at the flat surface because of the Laplace pressure, as described by Kelvin's equation. An experimental system for measuring water evaporation in extended-nanospaces was developed which can strictly control equilibrium vapor pressure and temperature in extended-nanochannels. The vapor pressures in extended-nanospaces were lower than those estimated from the bulk theory and Kelvin's equation.[67]

Liquid Model. In order to explain liquid properties in extended-nanospaces, the effects of the electric double-layer, i.e., a classical model of solid−liquid interfaces, have been considered. The EDL is formed by counterions in electrolyte solutions attracted to the charged solid surface (Figure 4a). In a typical model, the EDL consists of the solid layer of adsorbed ions, with a thickness on the order of 1 Å, and the diffuse layer of ions under the electrostatic force described by the Poisson−Boltzmann equation. The thickness of the EDL is approximately determined by the Debye length and depends on the electrolyte concentration. In extended-nanospaces, the EDL thickness is in the range of 1−100 nm.

On the basis of the EDL model, extended-nanospaces are considered to be filled entirely with the diffuse layer. This partially explains the reported liquid properties. Previously, the effects of EDL overlap in extended-nanochannels have been investigated.[31,55−57,60,68−71] Excess counterions can increase the liquid conductivity, and the apparent viscosity is affected by the streaming potential. The streaming potential inverse to the flow direction electrically drives the ions, and the fluid flow is suppressed by the ion drag; this is called the electroviscous effect. However, the experimental results are partially inconsistent with the results of numerical simulations based on the EDL model.[56,57,68,69,72] In the conventional EDL model, which considers the ion distribution in bulk solutions, the entirety of the unique liquid properties in extended-nanospaces cannot be explained, especially the unique proton behaviors mentioned above.

On the other hand, from the results of NMR measurements, Kitamori et al. proposed a model of aqueous liquids with a heterogeneous structure; this is the three-phase model illustrated in Figure 4b.[64] In this model, three phases of water are considered: the adsorption phase, the proton transfer phase, and the bulk phase. In the bulk phase, the water molecules have an ordinary liquid structure and freely translate and rotate. In the adsorption phase, the water has an ice-like structure in which both translation and rotation are inhibited. Intermediate to the adsorption phase and the bulk phase, a proton transfer phase of approximately 50 nm thickness exists and features loosely coupled water molecules that keep a four-coordinated H_2O structure, have slower translational motions, and possess high proton transfer capabilities resulting from proton hopping along a linear O···H−O hydrogen bonding chain. The thickness of the proton transfer phase was determined based on the channel-size dependency of the spin−lattice relaxation rate (^{1}H $1/T_1$) of water, which reflects the motion of water molecules.[12] The ^{1}H $1/T_1$ increased with decreasing channel size below 1000 nm, and this indicates slower motion of water molecules. The ^{1}H $1/T_1$ reaches a plateau in the channel size range from 50 to 200 nm. The ^{1}H $1/T_1$ again increases with decreasing the channel size smaller than 50 nm. This plateau suggests that the channel is filled only by the proton transfer phase at around 50 nm thickness. For the channels smaller than 50 nm, the molecular motion is further inhibited because the adsorption phase becomes dominant. As suggested from the results of NMR measurements, the three phase model can be predicted experimentally.

On the basis of the three phase model of heterogeneous liquid structure, the effects of the proton transfer phase are expected to be dominant in extended-nanospaces. Many of the unique liquid properties attributed to the water structure and proton behavior can be described and experimentally observed, as described above. However, liquid structures featuring loosely coupled water molecules within 50 nm of the surface have not been directly observed. In addition, the formation mechanism of the proton transfer phase, whose thickness is much larger than the molecular scale, is still unknown.

On the basis of these liquid models, the relationship between the EDL and extended-nanoscale heterogeneous liquids is an important outstanding issue whose resolution is required to explain the unique liquid properties in extended-nano spaces. Using the hydrogen ion distribution in an extended-nanochannel obtained by STED microscopy, the effects of these unique liquid properties were studied by numerical simulation. It is found that the lower dielectric constant of water in extended-nanospaces affects the distribution of hydrogen ions, regarded as the electric double layer.[73,74] Further research will provide more general liquid models which can explain the principle behind these unique liquid properties.

Establishing models for liquids in extended-nanospaces is important in the design of novel extended-nanofluidic devices. The effects of pH, electrolyte concentration, and electrolyte composition on the liquid properties, especially, must be taken into account, since it is well-known that the EDL is significantly affected by these parameters. pH affects the surface dissociation, and the electrolyte concentration and composition affect the Debye length of the double layer. These result in changes to the liquid properties related to the double layer, such as the electrical conductance, the liquid viscosity (via the electroviscous effect), and the apparent diffusion (related to the surface electrostatic effect). On the other hand, the influence of these parameters on the proton transfer phase has not yet been revealed. Currently, our group has initial results suggesting that the electrolyte composition can affect the proton transfer phase by ion hydration, resulting in changes in the liquid properties such as the viscosity and the diffusion coefficient.[75]

■ DEVICE TECHNOLOGIES FOR CHEMISTRY AND BIOLOGY

By exploiting the unique properties of extended-nanospaces mentioned above, novel functional devices never before realized using microspaces were developed. The smallness of the extended-nanospaces, with dimensions on the 10−100 nm scale and with attoliter to femtoliter volumes, is highly suitable for the manipulation of biomolecules. The surface effects dominant in extended-nanospaces, such as electrostatic and hydrophobic/hydrophilic interactions, have been applied to the separation and concentration of molecules. Furthermore, more general chemical analyses and processing techniques have been proposed that integrate top-down and bottom-up fabrication and fluidic control methods. In this section, we introduce the various functional devices, focusing on those in which the unique properties are utilized.

Needless to say, the small size of extended-nanospaces is important for analytical devices. Because the extended-nanospace is smaller than a single cell (and comparable in size to

dx.doi.org/10.1021/ac4026303 | Anal. Chem. 2014, 86, 4068−4077

mitochondria), a local electroporation device for single cell[76] and an analytical device for mitochondria[77] were developed. The behaviors of biopolymers, as represented by DNA, in extended-nanochannels have been intensively investigated. When a DNA molecule is introduced into an extended-nanochannel electrophoretically, the DNA molecule is stretched by electric repulsion with the nanochannel surface.[78] This effect is exploited in many analytical devices involving DNA, including epigenetic analysis,[38] denaturation mapping,[79] and next-generation DNA sequencing.[46] In addition, separation of DNA in extended-nanospaces was implemented with the help of nanostructures, such as nanopillars,[13] and entropic effects.[7,80] The EDL effect also becomes obvious in extended-nanospaces. When the thickness of the EDL, represented by Debye length, is similar to the depth of the extended-nanospace, an EDL overlap appears, and the extended-nanochannel operates as a filter, passing ions with a specific charge. Rectification devices called nanofluidic diodes[9] have been developed using this ion exchange effect and implemented in applications such as biomolecule sensing,[81] energy harvesting,[82] and biomimetic ion pumps.[83] In addition, preconcentration,[8] isoelectric focusing,[84] and isotachophoresis[85] devices were developed utilizing the EDL effect.

Although these nanochannels and nanostructures were fabricated using only top-down technologies, integration with bottom-up technologies allows more sophisticated chemical functions. For example, an immunoassay device was developed that immobilizes antibody molecules on extended-nanochannel walls using bottom-up surface modification techniques and low-temperature bonding.[86] In a conventional immunoassay using a 96-well microtiter plate, an antibody is immobilized on the bottom of the plate to capture antigen molecules in the wells. This results in very low capture efficiency and an analysis time of several hours to 1 day because the size of the well (millimeter scale) is comparable to the distance that the antigen molecules move in several hours by diffusion. Microfluidic immunoassays that shorten the analysis times to minutes have been developed,[87] although the capture efficiency is still low (~0.1%). Extended-nanoimmunoassay techniques can dramatically improve the capture efficiency because the size of the extended-nanochannel is much smaller than the distance that the antigen molecule moves in a few seconds by diffusion. Therefore, the extended-nanoimmunoassay is expected to provide a sensitive analytical tool for single cell.

The development of fluidic control techniques also makes possible more general analytical techniques, such as chromatography. Chromatography is one of the most robust techniques to separate molecules by surface interactions. In conventional liquid chromatography, separation columns packed with porous particles have been generally used to enhance these interactions. However, the packed column has a limited separation efficiency for the following reasons: First, as shown in Figure 5a, unwanted diffusion (so-called "eddy diffusion") occurs as a result of the nonuniform spaces and pathways of analyte molecules. Second, transport of the analyte molecules into pores where surface interactions mainly occur is slow and uneven because of the micrometer-scale particles. In contrast, when an extended-nanochannel is used as a separation column, the straight nanochannel eliminates eddy diffusion and produces faster mass transfer and enhanced surface interactions with the analyte molecules, as shown in Figure 5b. Therefore, the separation efficiency of extended-nanochromatography is theoretically higher than that in a conventional packed column

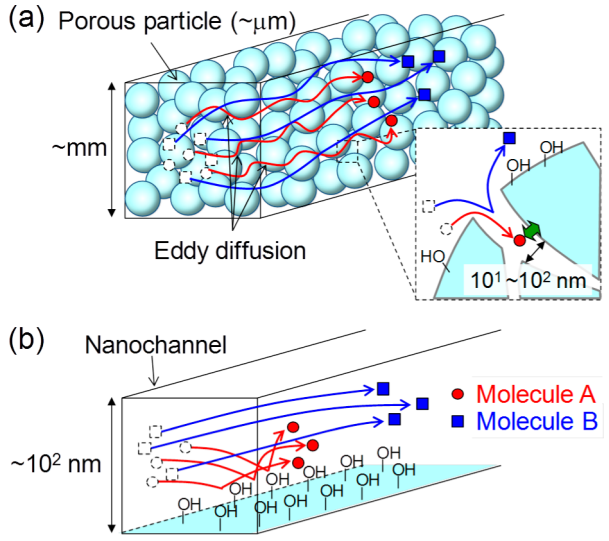

Figure 5. Concept of (a) conventional packed chromatographic column and (b) extended-nanochromatography.

by 2 orders of magnitude. Thus, analytical devices realizing incomparable efficiencies, as well as requiring extremely small sample volumes, were developed using extended-nanospaces.[88]

More interesting are devices utilizing the unique liquid properties present in extended-nanospaces, such as fuel cell devices that exploit high proton conductivity.[89,90] In a conventional fuel cell, an external fuel supply is indispensable, and the degradation of the proton exchange membrane (PEM) results in a performance decrease. To solve these problems, a light fuel cell incorporating a fuel generator by integrating top-down and bottom-up technologies was proposed. The device consists of a photocatalyst and electrodes integrated in microchannels and extended-nanochannels bridging the microchannels, as shown in Figure 6. In the fuel generator part, water

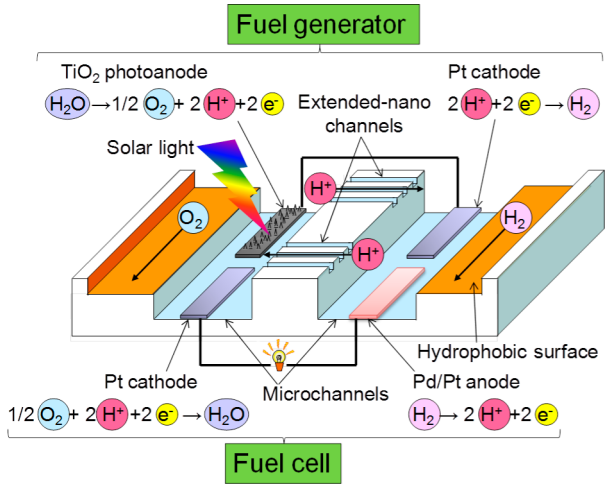

Figure 6. Concept of light-driven micro fuel cell device.

is split into oxygen and protons by photocatalytic reactions, and the protons are used to generate hydrogen. Simultaneously, in the fuel cell part, hydrogen is oxidized to generate electric current and water. For both the fuel generator and fuel cell, the extended-nanochannel works as a highly conductive proton transport media that is more robust than conventional polymer PEMs. In addition, the oxygen and hydrogen produced in the

dx.doi.org/10.1021/ac4026303 | Anal. Chem. 2014, 86, 4068−4077

fuel generator are removed immediately into a shallow microchannel with hydrophobic modifications and supplied to the fuel cell. This makes autonomous driving by only light and water possible. Other devices exploiting the unique liquid properties, such as decreased saturated vapor pressure and accelerated condensation, are anticipated for distillation[91] purposes.

CONCLUSION AND FUTURE PERSPECTIVES

State-of-the-art extended-nanofluidic principles and devices are systematically described. On the basis of fundamental technologies and recently discovered unique liquid properties, novel extended-nano fluidic devices are being developed for the biochemical analysis of countable numbers of macromolecules, ultrahigh efficiency separation, and energy harvesting. Since the extended-nanospaces also exist in porous media, synaptic clefts, and mitochondria in biological systems, the science of these unique liquid properties will greatly contribute to fields such as geoscience, separation science, and biology.

For these discoveries and devices to profoundly affect the fluid engineering field, there are still several issues that need to be resolved. For fundamental technologies, fluidic control methods such as open/close valves and the formation of multiphase flows are required to realize integration for general chemical operations. For extended-nanospace science, an important issue is to clarify the mechanisms underlying the unique liquid properties and establish a general liquid model. The development of applications for extended-nanospaces will be based on these integration methods and the general liquid model. Cost-effective and scalable nanochannel fabrication and surface modification/washing will be challenging topics for emerging device applications.

AUTHOR INFORMATION

Corresponding Author

*Phone: +81-3-5841-7231. Fax: +81-3-5841-6039. E-mail: kitamori@icl.t.u-tokyo.ac.jp.

Notes

The authors declare no competing financial interest.

Biographies

Kazuma Mawatari received his Ph.D. from the University of Tokyo and is currently an associate professor at the University of Tokyo, Department of Applied Chemistry and Bioengineering. His research is focused on ultrasensitive laser spectroscopy and integration of the analytical system in the micro/nano space. He is the coauthor of more than 75 international papers, and most of his recent publications are related to nanofluidics and devices.

Yutaka Kazoe is an assistant professor of Applied Chemistry at the University of Tokyo. He received his Ph.D. degree from Keio University and has been a Visiting Scholar at Georgia Institute of Technology. He has been teaching at the University of Tokyo since 2011. The main objects of his research are micro/nanoscale fluid flows and micro/nanofluidics. He has developed super-resolution optical methodologies for measuring micro/nanoscale fluid flows and focuses on fluid behavior near interfaces.

Hisashi Shimizu received his Ph.D. from the University of Tokyo and is currently an assistant professor at the University of Tokyo, Department of Applied Chemistry. His research is focused on highly sensitive detection methods, especially for nonfluorescent molecules based on photothermal spectroscopy and micro/nanofluidic analytical devices such as chromatography.

Yuriy Pihosh received his Ph.D at the Charles University in Prague and presently holds the position of a Senior Researcher at the University of Tokyo, Department of Applied Chemistry and Bioengineering. His research mostly concentrates on semiconductor photoelectrochemistry for solar energy conversion and storage. He is currently working on the creation of a light driven microfuel cell device that would utilize specific properties of micro and extended-nano spaces.

Takehiko Kitamori received his Ph.D. from the University of Tokyo and is currently a professor at the University of Tokyo, Department of Applied Chemistry and Bioengineering. He has pioneered micro/nanofluidic research in Japan and is the inventor of thermal lens microscopy (TLM). He is the coauthor of more than 240 international papers. He has recently been taking great interest in extended nanospace, defined as 10−100 nm, and is currently exploring new phenomena and technology in this area.

REFERENCES

(1) Reyes, D.; Iossifidis, D.; Auroux, P.; Manz, A. *Anal. Chem.* **2002**, *74*, 2623−2636.
(2) Tokeshi, M.; Minagawa, T.; Uchiyama, K.; Hibara, A.; Sato, K.; Hisamoto, H.; Kitamori, T. *Anal. Chem.* **2002**, *74*, 1565−1571.
(3) Gunther, A.; Jensen, K. F. *Lab Chip* **2006**, *6*, 1487−1503.
(4) Ohashi, T.; Mawatari, K.; Kitamori, T. *Biomicrofluidics* **2010**, *4*, 032207.
(5) Taniguchi, K.; Kajiyama, T.; Kambara, H. *Nat. Methods* **2009**, *6*, 503−506.
(6) Riehn, R.; Lu, M.; Wang, Y.; Lim, S.; Cox, E.; Austin, R. *Proc. Natl. Acad. Sci. U.S.A.* **2005**, *102*, 10012−10016.
(7) Fu, J.; Schoch, R. B.; Stevens, A. L.; Tannenbaum, S. R.; Han, J. *Nat. Nanotechnol.* **2007**, *2*, 121−128.
(8) Wang, Y.; Stevens, A.; Han, J. *Anal. Chem.* **2005**, *77*, 4293−4299.
(9) Karnik, R.; Duan, C.; Castelino, K.; Daiguji, H.; Majumdar, A. *Nano Lett.* **2007**, *7*, 547−551.
(10) Tsukahara, T.; Mawatari, K.; Kitamori, T. *Chem. Soc. Rev.* **2010**, *39*, 1000−1013.
(11) Mawatari, K.; Tsukahara, T.; Sugii, Y.; Kitamori, T. *Nanoscale* **2010**, *2*, 1588−1595.
(12) Tsukahara, T.; Mizutani, W.; Mawatari, K.; Kitamori, T. *J. Phys. Chem. B* **2009**, *113*, 10808−10816.
(13) Kaji, N.; Tezuka, Y.; Takamura, Y.; Ueda, M.; Nishimoto, T.; Nakanishi, H.; Horiike, Y.; Baba, Y. *Anal. Chem.* **2004**, *76*, 15−22.
(14) Wang, Y.; Tegenfeldt, J.; Reisner, W.; Riehn, R.; Guan, X.; Guo, L.; Golding, I.; Cox, E.; Sturm, J.; Austin, R. *Proc. Natl. Acad. Sci. U.S.A.* **2005**, *102*, 9796−9801.
(15) Guo, L.; Cheng, X.; Chou, C. *Nano Lett.* **2004**, *4*, 69−73.
(16) Sivanesan, P.; Okamoto, K.; English, D.; Lee, C.; DeVoe, D. *Anal. Chem.* **2005**, *77*, 2252−2258.
(17) Zhang, L.; Gu, F.; Tong, L.; Yin, X. *Microfluid. Nanofluid.* **2008**, *5*, 727−732.
(18) Wang, X.; Ge, L.; Lu, J.; Li, X.; Qiu, K.; Tian, Y.; Fu, S.; Cui, Z. *Microelectron. Eng.* **2009**, *86*, 1347−1349.
(19) Kovarik, M. L.; Jacobson, S. C. *Anal. Chem.* **2006**, *78*, 5214−5217.
(20) Renberg, B.; Sato, K.; Tsukahara, T.; Mawatari, K.; Kitamori, T. *Microchim. Acta* **2009**, *166*, 177−181.
(21) Renberg, B.; Sato, K.; Mawatari, K.; Idota, N.; Tsukahara, T.; Kitamori, T. *Lab Chip* **2009**, *9*, 1517−1523.
(22) Xu, Y.; Wang, C.; Li, L.; Matsumoto, N.; Jang, K.; Dong, Y.; Mawatari, K.; Suga, T.; Kitamori, T. *Lab Chip* **2013**, *13*, 1048−1052.
(23) Tegenfeldt, J.; Prinz, C.; Cao, H.; Chou, S.; Reisner, W.; Riehn, R.; Wang, Y.; Cox, E.; Sturm, J.; Silberzan, P.; Austin, R. *Proc. Natl. Acad. Sci. U.S.A.* **2004**, *101*, 10979−10983.
(24) Garcia, A.; Ista, L.; Petsev, D.; O'Brien, M.; Bisong, P.; Mammoli, A.; Brueck, S.; Lopez, G. *Lab Chip* **2005**, *5*, 1271−1276.
(25) Vlassiouk, I.; Smirnov, S.; Siwy, Z. *Nano Lett.* **2008**, *8*, 1978−1985.
(26) Abgrall, P.; Nguyen, N. T. *Anal. Chem.* **2008**, *80*, 2326−2341.

(27) Desmet, G.; Baron, G. *Anal. Chem.* **2000**, *72*, 2160−2165.
(28) Clicq, D.; Pappaert, K.; Vankrunkelsven, S.; Vervoort, N.; Baron, G.; Desmet, G. *Anal. Chem.* **2004**, *76*, 430A−438A.
(29) Vankrunkelsven, S.; Clicq, D.; Cabooter, D.; De Malsche, W.; Gardeniers, J.; Desmet, G. *J. Chromatogr., A* **2006**, *1102*, 96−103.
(30) Hibara, A.; Saito, T.; Kim, H.; Tokeshi, M.; Ooi, T.; Nakao, M.; Kitamori, T. *Anal. Chem.* **2002**, *74*, 6170−6176.
(31) Tas, N.; Haneveld, J.; Jansen, H.; Elwenspoek, M.; van den Berg, A. *Appl. Phys. Lett.* **2004**, *85*, 3274−3276.
(32) Tamaki, E.; Hibara, A.; Kim, H.; Tokeshi, M.; Kitamori, T. *J. Chromatogr., A* **2006**, *1137*, 256−262.
(33) Tsukahara, T.; Mawatari, K.; Hibara, A.; Kitamori, T. *Anal. Bioanal. Chem.* **2008**, *391*, 2745−2752.
(34) Ishibashi, R.; Mawatari, K.; Takahashi, K.; Kitamori, T. *J. Chromatogr., A* **2012**, *1228*, 51−56.
(35) Kojima, R.; Mawatari, K.; Renberg, B.; Tsukahara, T.; Kitamori, T. *Microchim. Acta* **2009**, *164*, 307−310.
(36) Kato, M.; Inaba, M.; Tsukahara, T.; Mawatari, K.; Hibara, A.; Kitamori, T. *Anal. Chem.* **2010**, *82*, 543−547.
(37) Dittrich, P.; Manz, A. *Anal. Bioanal. Chem.* **2005**, *382*, 1771−1782.
(38) Cipriany, B. R.; Zhao, R.; Murphy, P. J.; Levy, S. L.; Tan, C. P.; Craighead, H. G.; Soloway, P. D. *Anal. Chem.* **2010**, *82*, 2480−2487.
(39) Kitamori, T.; Tokeshi, M.; Hibara, A.; Sato, K. *Anal. Chem.* **2004**, *76*, 52A−60A.
(40) Shimizu, H.; Mawatari, K.; Kitamori, T. *Anal. Chem.* **2010**, *82*, 7479−7484.
(41) Ly, N.; Foley, K.; Tao, N. *Anal. Chem.* **2007**, *79*, 2546−2551.
(42) Oh, Y.; Park, S.; Kang, M.; Choi, J.; Nam, Y.; Jeong, K. *Small* **2011**, *7*, 184−188.
(43) Schoch, R. B.; Cheow, L. F.; Han, J. *Nano Lett.* **2007**, *7*, 3895−3900.
(44) Kasianowicz, J.; Brandin, E.; Branton, D.; Deamer, D. *Proc. Natl. Acad. Sci. U.S.A.* **1996**, *93*, 13770−13773.
(45) Liang, X.; Chou, S. Y. *Nano Lett.* **2008**, *8*, 1472−1476.
(46) McGinn, S.; Gut, I. G. *New Biotechnol.* **2013**, *30*, 366−372.
(47) Kazoe, Y.; Mawatari, K.; Sugii, Y.; Kitamori, T. *Anal. Chem.* **2011**, *83*, 8152−8157.
(48) Haneveld, J.; Tas, N. R.; Brunets, N.; Jansen, H. V.; Elwenspoek, M. *J. Appl. Phys.* **2008**, *104*, 014309.
(49) Li, L.; Kazoe, Y.; Mawatari, K.; Sugii, Y.; Kitamori, T. *J. Phys. Chem. Lett.* **2012**, *3*, 2447−2452.
(50) Plecis, A.; Schoch, R.; Renaud, P. *Nano Lett.* **2005**, *5*, 1147−1155.
(51) Pappaert, K.; Biesemans, J.; Clicq, D.; Vankrunkelsven, S.; Desmet, G. *Lab Chip* **2005**, *5*, 1104−1110.
(52) Schoch, R.; Bertsch, A.; Renaud, P. *Nano Lett.* **2006**, *6*, 543−547.
(53) Durand, N. F. Y.; Bertsch, A.; Todorova, M.; Renaud, P. *Appl. Phys. Lett.* **2007**, *91*, 203106.
(54) Whitby, M.; Cagnon, L.; Thanou, M.; Quirke, N. *Nano Lett.* **2008**, *8*, 2632−2637.
(55) Stein, D.; Kruithof, M.; Dekker, C. *Phys. Rev. Lett.* **2004**, *93*, 035901.
(56) Lee, C.; Joly, L.; Siria, A.; Biance, A.; Fulcrand, R.; Bocquet, L. *Nano Lett.* **2012**, *12*, 4037−4044.
(57) Duan, C.; Majumdar, A. *Nat. Nanotechnol.* **2010**, *5*, 848−852.
(58) Liu, S.; Pu, Q.; Gao, L.; Korzeniewski, C.; Matzke, C. *Nano Lett.* **2005**, *5*, 1389−1393.
(59) Tsukahara, T.; Kuwahata, T.; Hibara, A.; Kim, H.; Mawatari, K.; Kitamori, T. *Electrophoresis* **2009**, *30*, 3212−3218.
(60) van der Heyden, F.; Stein, D.; Dekker, C. *Phys. Rev. Lett.* **2005**, *95*, 116104.
(61) Xie, Y.; Wang, X.; Xue, J.; Jin, K.; Chen, L.; Wang, Y. *Appl. Phys. Lett.* **2008**, *93*, 163116.
(62) Morikawa, K.; Mawatari, K.; Kato, M.; Tsukahara, T.; Kitamori, T. *Lab Chip* **2010**, *10*, 871−875.
(63) Morikawa, K.; Kazoe, Y.; Mawatari, K.; Tsukahara, T.; Kitamori, T. *Proc. MicroTAS 2012* **2012**, *1*, 701−703.
(64) Tsukahara, T.; Hibara, A.; Ikeda, Y.; Kitamori, T. *Angew. Chem., Int. Ed.* **2007**, *46*, 1180−1183.
(65) Chinen, H.; Mawatari, K.; Pihosh, Y.; Morikawa, K.; Kazoe, Y.; Tsukahara, T.; Kitamori, T. *Angew. Chem., Int. Ed.* **2012**, *51*, 3573−3577.
(66) Morikawa, K.; Mawatari, K.; Kazoe, Y.; Tsukahara, T.; Kitamori, T. *Appl. Phys. Lett.* **2011**, *99*, 123115.
(67) Tsukahara, T.; Maeda, T.; Hibara, A.; Mawatari, K.; Kitamori, T. *RSC Adv.* **2012**, *2*, 3184−3186.
(68) Phan, V.; Yang, C.; Nguyen, N. *Microfluid. Nanofluid.* **2009**, *7*, 519−530.
(69) Mortensen, N. A.; Kristensen, A. *Appl. Phys. Lett.* **2008**, *92*, 063110.
(70) Pennathur, S.; Santiago, J. *Anal. Chem.* **2005**, *77*, 6772−6781.
(71) Pennathur, S.; Santiago, J. *Anal. Chem.* **2005**, *77*, 6782−6789.
(72) Anzo, K.; Okada, T. *Anal. Chem.* **2012**, *84*, 10852−10854.
(73) Kazoe, Y.; Chang, C.; Mawatari, K.; Kitamori, T. *Anal. Chem.* **2012**, *84*, 10855−10855.
(74) Chang, C.; Kazoe, Y.; Morikawa, K.; Mawatari, K.; Yang, R.; Kitamori, T. *Anal. Chem.* **2013**, *85*, 4468−4474.
(75) Kasai, K.; Kazoe, Y.; Morikawa, K.; Mawatari, K.; Kitamori, T. *Proc. MicroTAS 2012* **2012**, *1*, 1285−1287.
(76) Boukany, P. E.; Morss, A.; Liao, W.; Henslee, B.; Jung, H.; Zhang, X.; Yu, B.; Wang, X.; Wu, Y.; Li, L.; Gao, K.; Hu, X.; Zhao, X.; Hemminger, O.; Lu, W.; Lafyatis, G. P.; Lee, L. J. *Nat. Nanotechnol.* **2011**, *6*, 747−754.
(77) Zand, K.; Pham, T.; Davila, A., Jr.; Wallace, D. C.; Burke, P. J. *Anal. Chem.* **2013**, *85*, 6018−6025.
(78) Reisner, W.; Morton, K.; Riehn, R.; Wang, Y.; Yu, Z.; Rosen, M.; Sturm, J.; Chou, S.; Frey, E.; Austin, R. *Phys. Rev. Lett.* **2005**, *94*, 196101.
(79) Reisner, W.; Larsen, N. B.; Silahtaroglu, A.; Kristensen, A.; Tommerup, N.; Tegenfeldt, J. O.; Flyvbjerg, H. *Proc. Natl. Acad. Sci. U.S.A.* **2010**, *107*, 13294−13299.
(80) Stavis, S. M.; Geist, J.; Gaitan, M.; Locascio, L. E.; Strychalski, E. A. *Lab Chip* **2012**, *12*, 1174−1182.
(81) Wen, L.; Sun, Z.; Han, C.; Imene, B.; Tian, D.; Li, H.; Jiang, L. *Chem.—Eur. J.* **2013**, *19*, 7686−7690.
(82) Wen, L.; Tian, Y.; Guo, Y.; Ma, J.; Liu, W.; Jiang, L. *Adv. Funct. Mater.* **2013**, *23*, 2887−2893.
(83) Zhang, H.; Hou, X.; Zeng, L.; Yang, F.; Li, L.; Yan, D.; Tian, Y.; Jiang, L. *J. Am. Chem. Soc.* **2013**, *135*, 16102−16110.
(84) Startsev, M. A.; Inglis, D. W.; Baker, M. S.; Goldys, E. M. *Anal. Chem.* **2013**, *85*, 7133−7138.
(85) Quist, J.; Vulto, P.; van der Linden, H.; Hankemeier, T. *Anal. Chem.* **2012**, *84*, 9065−9071.
(86) Shirai, K.; Mawatari, K.; Kitamori, T. *Proc. MicroTAS 2012* **2012**, *1*, 713−715.
(87) Sato, K.; Tokeshi, M.; Odake, T.; Kimura, H.; Ooi, T.; Nakao, M.; Kitamori, T. *Anal. Chem.* **2000**, *72*, 1144−1147.
(88) Ishibashi, R.; Mawatari, K.; Kitamori, T. *Small* **2012**, *8*, 1237−1242.
(89) Pihosh, Y.; Mawatari, K.; Turkevych, I.; Le, T. H. H.; Kajita, Y.; Chinen, H.; Tosa, M.; Kitamori, T. *Proc. MicroTAS 2012* **2012**, *1*, 148−150.
(90) Kajita, Y.; Pihosh, Y.; Mawatari, K.; Kitamori, T. *Proc. MicroTAS 2012* **2012**, *1*, 2005−2007.
(91) Hibara, A.; Toshin, K.; Tsukahara, T.; Mawatari, K.; Kitamori, T. *Chem. Lett.* **2008**, *37*, 1064−1065.

■ NOTE ADDED AFTER ASAP PUBLICATION

This paper was published ASAP on April 1, 2014 with errors in the reference citations in Table 1. The corrected manuscript was reposted on April 17, 2014.